

**Chemoselective Polymerizations from Mixtures of Epoxide, Lactone,
Anhydride and CO₂**

Charles Romain,^{†*} Yunqing. Zhu,[†] Paul Dingwall,[†] Shyeni Paul,[†] Henry Rzepa,[†]
Antoine Buchard[‡] and Charlotte K. Williams^{†*}

[†]: Department of Chemistry, Imperial College London, London SW7 2AZ, UK

[‡]: Department of Chemistry, University of Bath, Bath BA2 7AY, UK

c.k.williams@imperial.ac.uk

Contents	Page #
Experimental Section	S2-S4
Table S1, Figure S1	S5
Figure S2	S6
Figure S3, Figure S4	S7
Figure S5, Figure S6	S8
Table S3	S9
Figure S7	S10
Table S4	S11
Figure S8	S12
Figure S9, Table S5	S13
Figure S10, Figure S11	S14
Figure S12, Figure S13	S15
Figure S14, Figure S15	S16
Figure S16, Figure S17	S17
Table S6, Figure S18	S18
Figure S19	S19
Figure S20	S20
Table S7, Table S8	S21
Data for Table1 (Figure S21-S29)	S22-25
Data for Table 2 (Figure S30-S34)	S26-28
References	S29

Complementary data available at <http://doi.org/10.14469/hpc/244>.

Experimental Section

General considerations

All polymerizations were performed under inert atmosphere using a Schlenk line and standard anaerobic techniques or in a dry, solvent-free glove-box. Catalyst **1** was prepared as described in the literature.¹ Toluene and THF were distilled, under an inert atmosphere, from sodium and were stored over activated 3 Å molecular sieves. CHO was received from Aldrich, dried over CaH₂ for a minimum of 48 h and fractionally distilled. ε-CL was dried over CaH₂ and fractionally distilled. Phthalic anhydride (Sigma) was purified by dissolution and filtration in dichloromethane (HPLC grade) and re-crystallized twice from hot toluene. After purification, both ε-CL and PA were stored in the glove-box.

Characterization Methods

NMR spectra were recorded on Bruker AVIII-400 and AVIII-500 spectrometers. All chemicals shifts were determined using residual signals of the deuterated solvents and were calibrated vs. SiMe₄. DOSY experiments were performed at a steady temperature of 298K with at least 32 gradient increments using the ledpgp2s sequence. Complete diffusion was ensured using the T1/T2 module of Topspin and DOSY transformations using either mono, bis- or tri-exponential fitting were performed using the same software after zero filling.

Size Exclusion Chromatography measurements were performed on a Polymer Laboratories PL-GPC 50 using THF at 1mL/min and 40 °C on two PLgel 5um MIXED-D column sets. Dual RID-MALLS detection was used using a Dawn 8+ MALLS detector (Wyatt) and the internal RID detector of the PL-50 system. Some of the SEC traces show 'shoulders' but in all cases the dispersities are <1.60. It is noted that the polymers likely feature both α-cyclohexyl-acetate, ω-hydroxyl and α,ω di-hydroxyl end-groups. The end-group characterization has been investigated in detail previously for catalyst **1**.²

In situ ATR-IR reaction monitoring were using a Mettler-Toledo ReactIR 4000 spectrometer equipped with a MCT detector and a silver halide DiComp probe.

Computational Details

DFT calculations were performed using Gaussian 09 (revision C01).³ Calculations used the ωB97XD density functional and the 6-31G(d) basis set. Self-consistent-reaction-cavity continuum solvation model was used with dichloromethane as the solvent to model solvation in cyclohexene oxide. All transition states were characterized by normal coordinate analysis revealing precisely one imaginary mode corresponding to the intended reaction. For **8PA'-TS** an IRC calculation was performed which also confirmed the identity of the transition state. Full coordinates for all the stationary points, together with normal mode animations are available via the Web-enhanced tables and which also include links to full details for each calculation found in a digital repository.

Typical Polymerization Procedures

Polymerizations of ε-CL in CHO (Table 1)

In a glovebox, the zinc catalyst (10.0 mg, 1.25×10^{-2} mmol), ε-CL (296 μL, 2.52 mmol) and CHO (1.02 mL, 10.1 mmol) were mixed in a screw-capped vial, charged with a stir bar (loading as described in Table 1). The mixture was then heated to 80 °C and left to react for the desired time (see Table 1).

Polymerizations of ε-CL in CHO with added CO₂ (Table 1)

In a glovebox, the zinc catalyst (10.00 mg, 1.25×10^{-2} mmol), ε-CL (1.08 mL, 7.50 mmol) and CHO (2.50 mL, 25.00 mmol) were mixed in Schlenk tube charged with a stir bar. Under a flow of nitrogen, the React-IR probe was introduced and the reaction was heated to 80 °C. As soon as the formation of PCL was observed, CO₂ was added to the reaction and the reaction was left at 80 °C for desired time.

Polymerizations of mixtures of ε -CL, PA and CHO (Table 2):

The zinc catalyst (10.0 mg, 1.25×10^{-2} mmol), phthalic anhydride (37.0 mg, 0.25 mmol) and ε -CL (210.0 μ L, 1.88 mmol) were dissolved in CHO (505.0 μ L, 5.00 mmol), under N₂ protection, in a screw-capped vial, charged with a stir bar. The mixture was then heated to 100 °C and left to react for 2 h. The block copolymer was precipitated using cold MeOH.

Polymerizations of ε -CL in CHO with added phthalic anhydride (Fig. S15)

In a glovebox, the zinc catalyst (20 mg, 2.50×10^{-2} mmol), ε -CL (1.78 mL, 15.00 mmol) and CHO (5.1 mL, 50.00 mmol) were mixed in Schlenk tube, charged with a stir bar. After 5 minutes, an aliquot was taken and phthalic anhydride (74.5 mg, 0.5 mmol) was added. The reaction was left to react and aliquots were taken after 20 minutes and 3 hours. No further formation of PCL was observed by ¹H NMR spectroscopy.

Table S1: The ROP of ε -CL attempted in the absence of CHO.

Entry	1/CHO/ ε -CL	t (h)	T (°C)	Solvent [ε -CL] ₀	ε -CL Conv. (%)
1	1/0/500	16	80	-	0
2	1/0/1000	24	130	-	0
3	1/0/100	5	80	Toluene (1M)	0

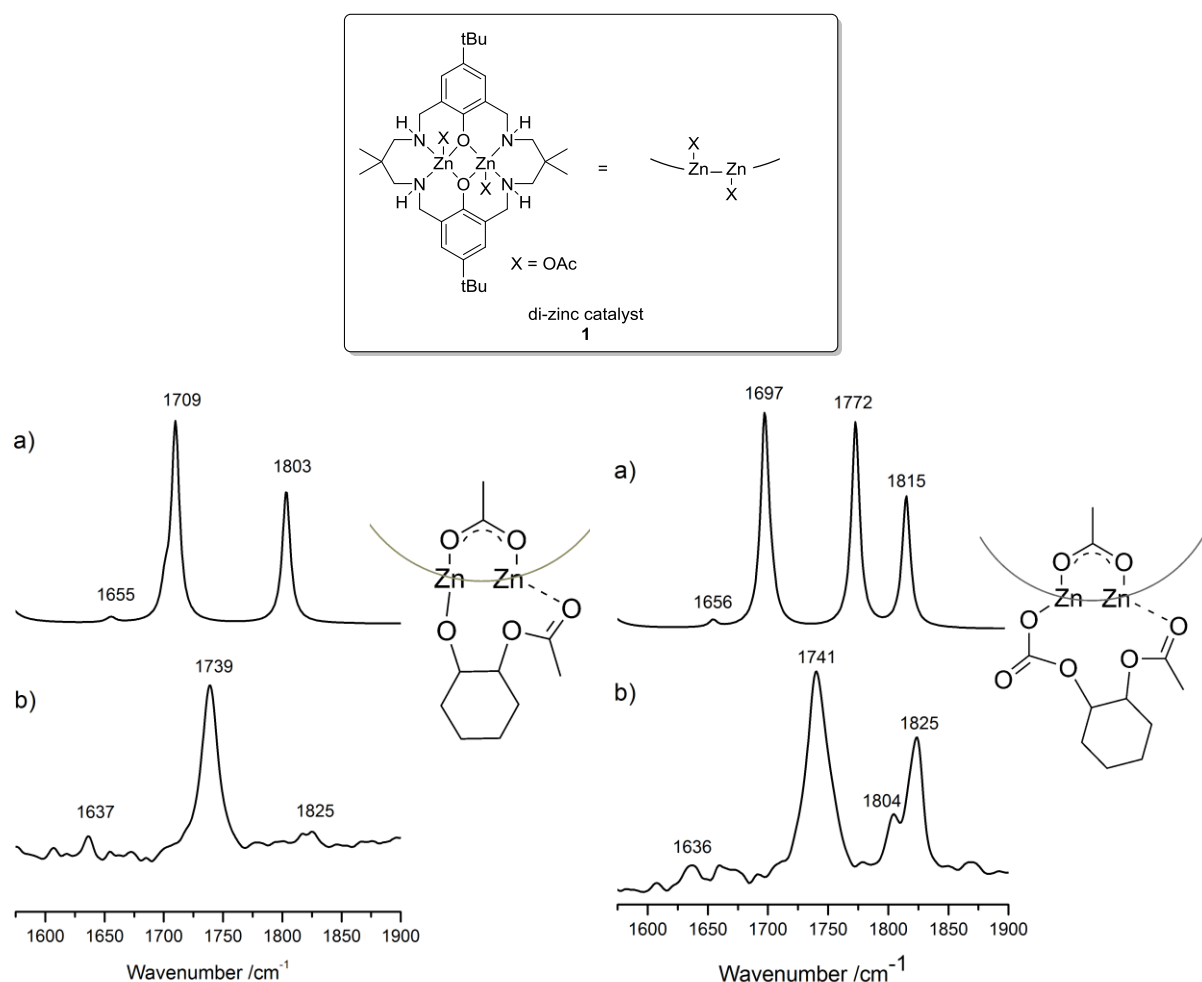


Figure S1: (Top) The structure of the di-zinc catalyst 1; (left) Intermediate formed after ring-opening of the CHO with acetate: (a) DFT calculated spectrum; (b) in situ spectrum measured using ATR-IR after 2 h at 80 °C. (right) Intermediate formed after sequential addition of CHO, then CO₂ (1 atm): (a) the DFT calculated spectrum after addition of CO₂ and (b) the in situ ATR-IR spectrum after addition of CO₂ (1 atm) for 14 h at 80 °C. Data reproduced with permission from the reference 4. Copyright 2015 American Chemical Society.

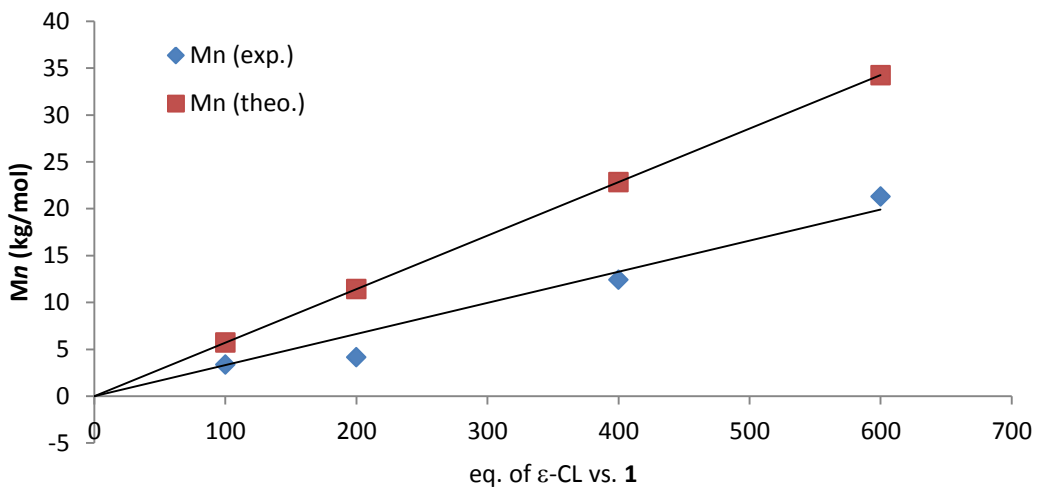


Figure S2: Plot showing linear fit between M_n and catalyst loading (Table S2, entries 1 to 4). The values for the M_n (experimental) (\diamond) were determined by SEC, calibrated with polystyrene standards, and a correction factor of 0.56 was applied as described in the literature.⁵ The values for the M_n (theoretical) (\blacksquare) were calculated in the following way: 1 (eq.) $\times \epsilon$ -CL (eq.) \times conversion $\times 114.14 \times (1/2)$.

Entry	1/CHO/ ϵ -CL	t (min)	ϵ -CL Conv. (%)	$M_{n(PS)}$ (D) kg.mol $^{-1}$	$M_{n(experimental)}$ kg.mol $^{-1}$	$M_{n(theoretical)}$ kg.mol $^{-1}$
1	1/900/100	40	100	6.0 (1.20)	3.4	5.7
2	1/800/200	45	100	7.4 (1.90)	4.1	11.4
3	1/600/400	40	100	22.2 (1.50)	12.4	22.8
4	1/400/600	35	100	38.0 (1.40)	21.3	34.2

Table S2: The data and conditions for the entries shown in Fig. S2.

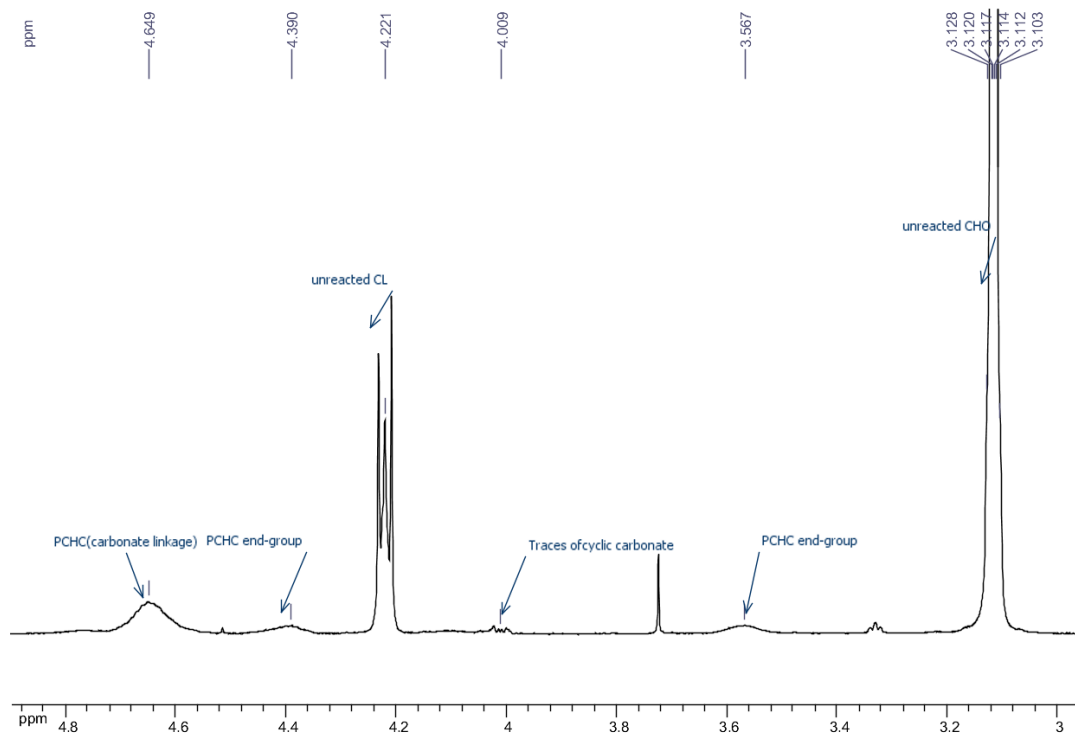


Figure S3: ^1H NMR spectrum showing formation of PCHC from a mixture **1**/CHO/ ε -CL/CO₂, the conditions are described in Table 1, entry 5.

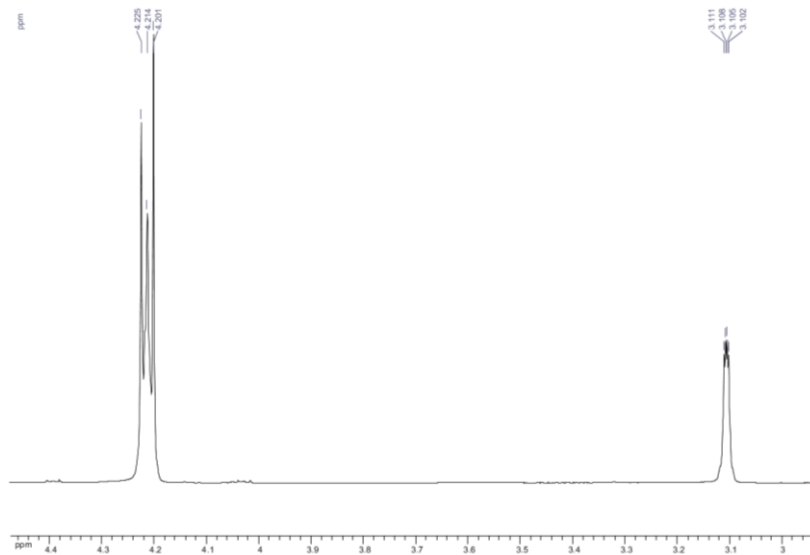


Figure S4: ^1H NMR spectrum (CDCl₃) of the product from Table 1, entry 7. Note that there is no formation of PCL or PCHC even after 8.5 h at 80 °C, under CO₂ atmosphere. Reaction conditions: **1**/CHO/ ε -CL/CO₂ = 1/400/600/1 atm.

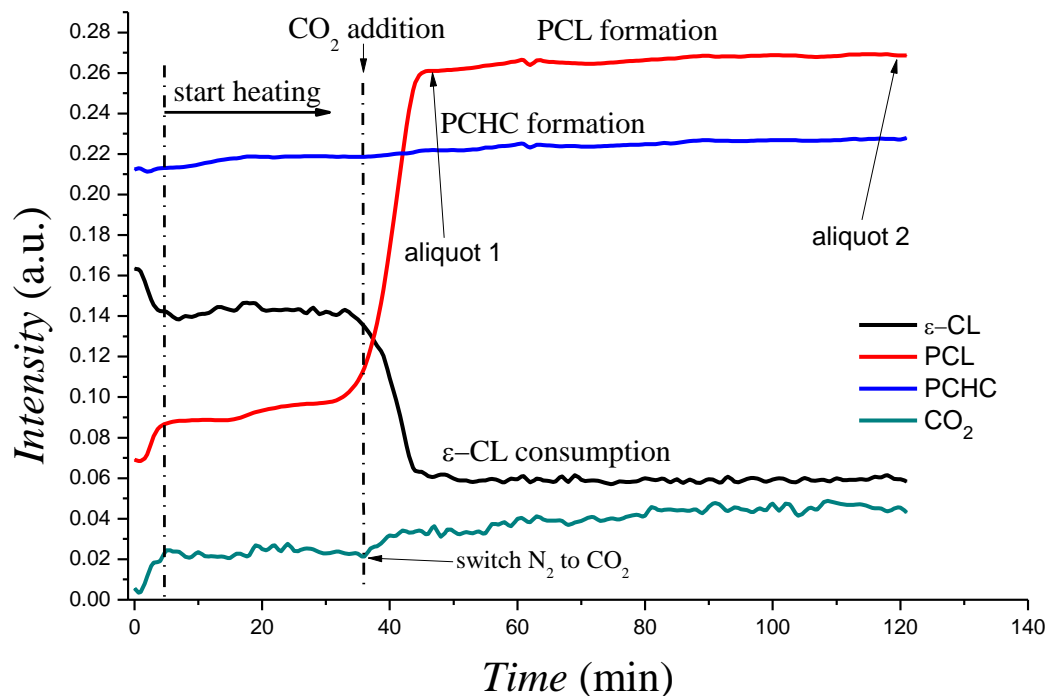


Figure S5: *In-situ* infrared spectroscopy showing the ROP of ε -CL where CO_2 is added (~ 37 mins) resulting in quenching of the polymerization. Reaction conditions: 80°C , $1/\text{CHO}/\varepsilon\text{-CL} = 1/600/2000$.

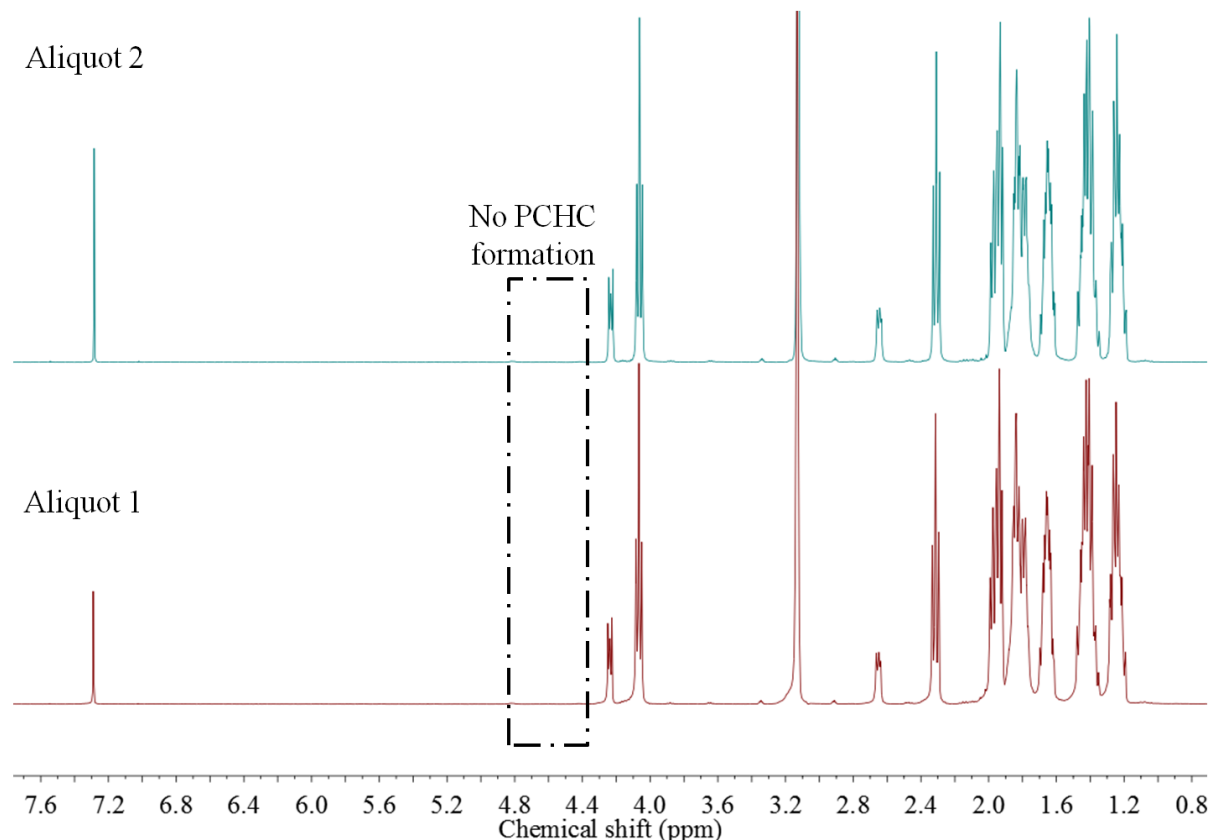


Figure S6: ^1H NMR spectrum of the sample resulting from the polymerization shown in Fig S5. Note that there is no formation of PCHC, even after prolonged time.

Table S3: Data for the DFT calculations illustrated in Figure 4.

Structure	Temperature	ΔG	JobID	Link
1	353.15	0.0	10005017	http://hdl.handle.net/10042/195777
2	353.15	-6.2	100085	http://hdl.handle.net/10042/195740
3	353.15	-2.7	100146	http://hdl.handle.net/10042/195741
4-TS	353.15	17.1	100086	http://hdl.handle.net/10042/195742
5	353.15	-10.7	100147	http://hdl.handle.net/10042/195743
6	353.15	-5.2	101999	http://hdl.handle.net/10042/195744
7 ^{CL}	353.15	-2.9	102000	http://hdl.handle.net/10042/195745
8 ^{CL} -TS	353.15	30.7	89629	http://hdl.handle.net/10042/195746
9 ^{CL}	353.15	-2.8	87244	http://hdl.handle.net/10042/195747
10 ^{CL} -TS	353.15	13.1	88875	http://hdl.handle.net/10042/195739
11 ^{CL}	353.15	9.4	89677	http://hdl.handle.net/10042/195748
12 ^{CL}	353.15	2.5	96988	http://hdl.handle.net/10042/195749
7 ^{CHO}	353.15	-5.7	103067	http://hdl.handle.net/10042/195750
8 ^{CHO} -TS	353.15	33.4	102869	http://hdl.handle.net/10042/195751
9 ^{CHO}	353.15	-22.1	103066	http://hdl.handle.net/10042/195752
7 ^{CO2}	353.15	-1.5	102925	http://hdl.handle.net/10042/195753
8 ^{CO2} -TS	353.15	7.5	102870	http://hdl.handle.net/10042/195754
9 ^{CO2}	353.15	6.1	102927	http://hdl.handle.net/10042/195755
10 ^{CO2} -TS	353.15	9.9	102871	http://hdl.handle.net/10042/195756
11 ^{CO2}	353.15	-6.5	103107	http://hdl.handle.net/10042/195757
12 ^{CO2}	353.15	-12.7	103702	http://hdl.handle.net/10042/195758

DFT protocol: # rwb97xd/6-31g(d) scrf=(cpccm,solvent=dichloromethane) NoSymm
temperature=353.15 K

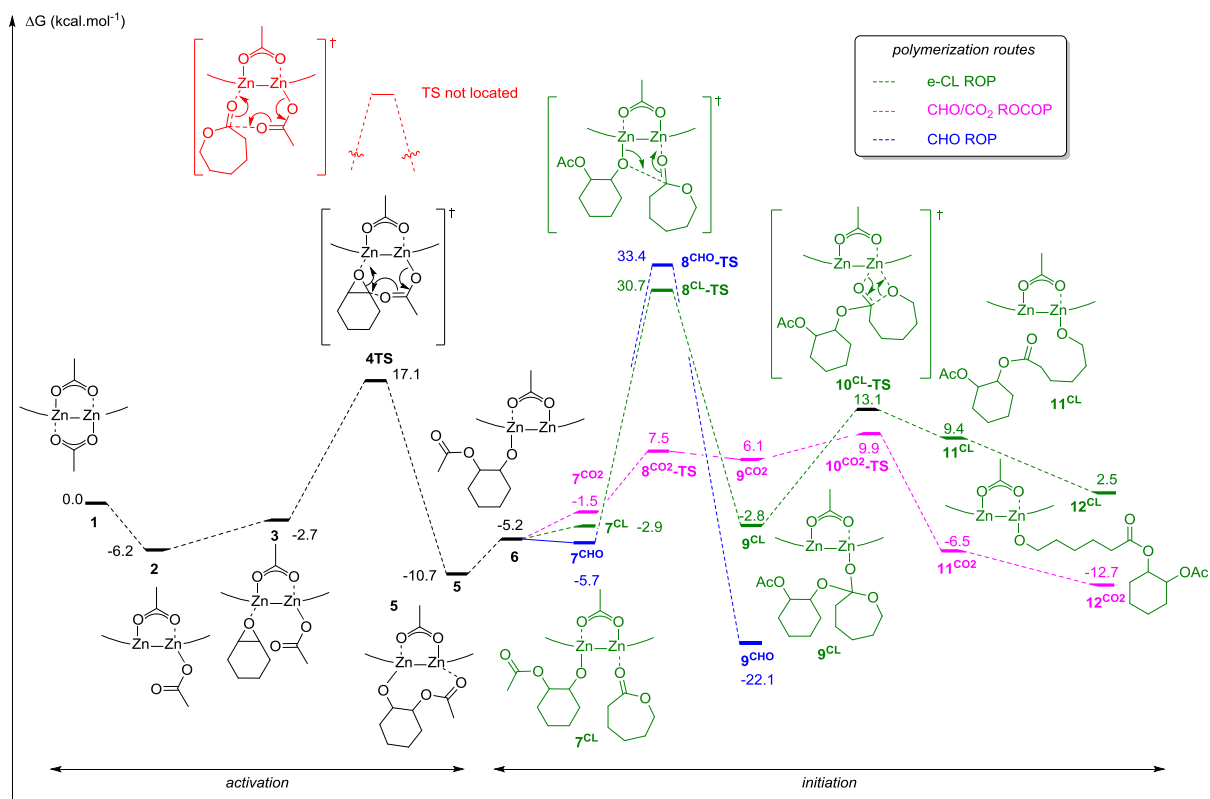


Figure S7: Potential energy surface for activation and initiation in ε -CL ROP (green); CHO/CO₂ ROCOP (purple) or CHO ROP (blue); DFT protocol: # rwb97xd/6-31g(d) scrf=(cpcm,solvent=dichloromethane) NoSymm temperature=353.15 K, as per Table S3. Data available at <http://doi.org/10.14469/hpc/275>.

Table S4: Data for the DFT calculations illustrated in Figure 5.

Structure	Temperature	ΔG	JobID	Link
12^{CL}	353.15	2.5	103108	http://hdl.handle.net/10042/196165
13^{CL}	353.155	-1.6	91950	http://hdl.handle.net/10042/195759
14^{CL-TS}	353.15	24.2	91635	http://hdl.handle.net/10042/195760
15^{CL}	353.15	2.3	93054	http://hdl.handle.net/10042/195761
16^{CL}	353.15	11.9	93885	http://hdl.handle.net/10042/195762
17^{CL}	353.15	5.1	94372	http://hdl.handle.net/10042/195763
18^{CL}	353.15	3.2	96333	http://hdl.handle.net/10042/195764
12^{CL}	353.15	2.5	96988	http://hdl.handle.net/10042/195749
13^{CHO}	353.15	2.3	90251	http://hdl.handle.net/10042/195765
14C^{HO-TS}	353.15	42.7	98840	http://hdl.handle.net/10042/195766
15^{CHO}	353.15	-8.9	99010	http://hdl.handle.net/10042/195767
12^{CL}	353.15	2.5	96988	http://hdl.handle.net/10042/195749
13^{CO2}	353.15	9.8	96987	http://hdl.handle.net/10042/195768
14C^{O2-TS}	353.15	10.9	98474	http://hdl.handle.net/10042/195769
15^{CO2}	353.15	9.9	98406	http://hdl.handle.net/10042/195770
16^{CO2-TS}	353.15	11.4	98232	http://hdl.handle.net/10042/195771
17^{CO2}	353.15	-9.2	98414	http://hdl.handle.net/10042/195772
18^{CO2}	353.15	-9.6	99732	http://hdl.handle.net/10042/195773
19^{CO2}	353.15	-7.6	99607	http://hdl.handle.net/10042/195774
20^{CO2}	353.15	17.7	99539	http://hdl.handle.net/10042/195775
21^{CO2}	353.15	-6.8	99608	http://hdl.handle.net/10042/195776

DFT protocol: # rwb97xd/6-31G(d) scrf=(cpccm,solvent=dichloromethane) NoSymm
temperature=353.15 K

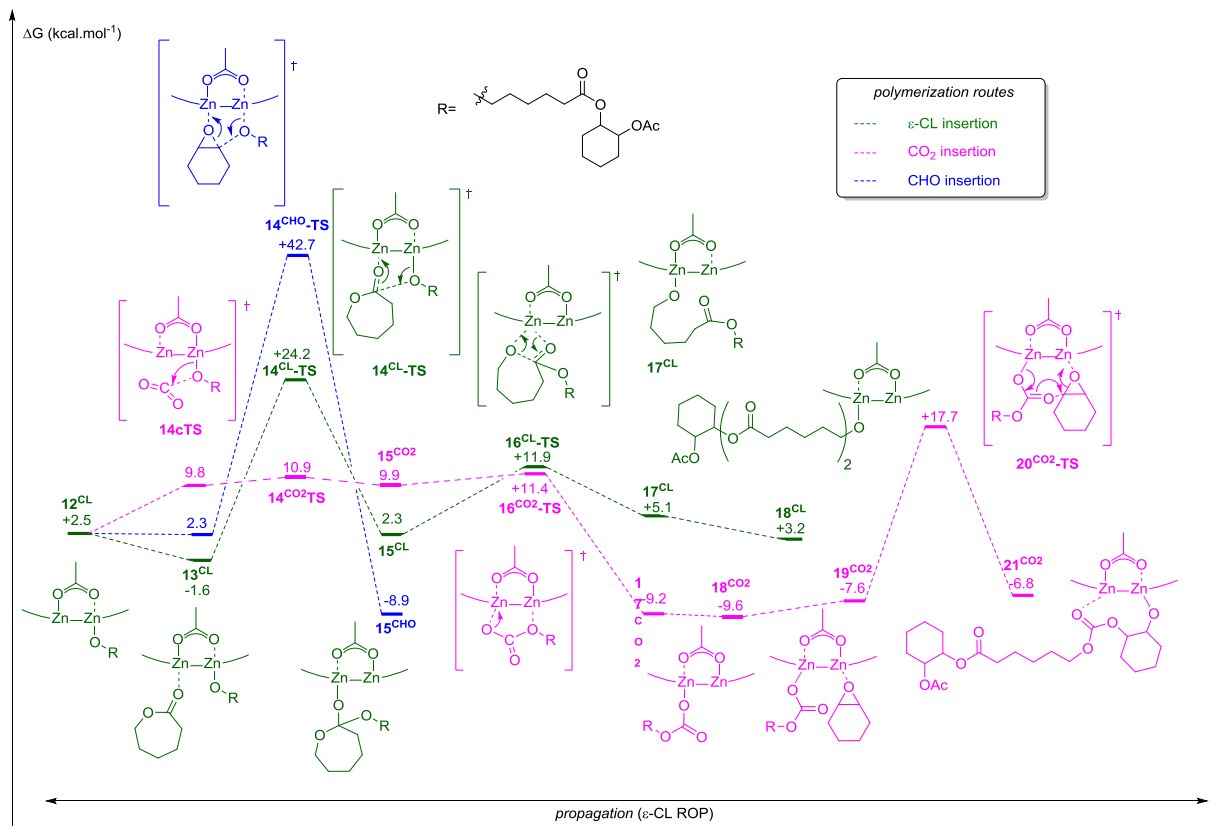


Figure S8: Potential energy surface for $\epsilon\text{-CL}$ propagation (green); CHO/ CO_2 ROCOP (purple) or CHO ROP (blue); DFT protocol: # rwb97xd/6-31g(d) scrf=(cpcm,solvent=dichloromethane) NoSymm temperature=353.15 K, as per Table S4. Data available at <http://doi.org/10.14469/hpc/278>.

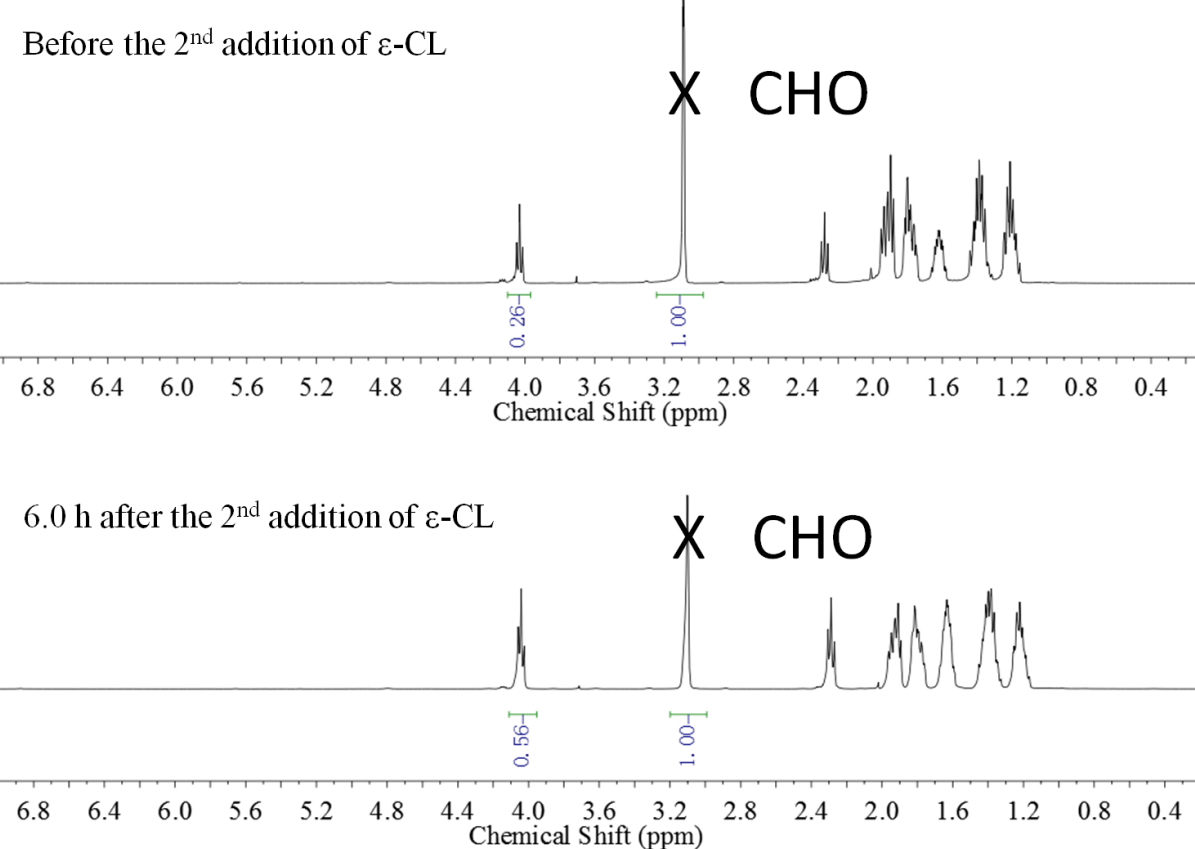


Figure S9: ^1H NMR spectrum of PCL before the 2nd addition of ε -CL (upper) and 6.0 h after the 2nd addition of ε -CL (lower) at room temperature. The signal of CHO is used as the internal reference.

#	[cat.]/[ε -CL]/[CHO]	Temp. (°C)	t (h)	M_n (kDa)	\bar{D}
a	1/100/900	80	2.0	8.8	1.43
b	1/(100+100)/900	25	6.0	18.1	1.49

Table S5: Data and conditions for the polymerizations monitored in Fig. S9. Full conversion of ε -CL was observed in all cases.

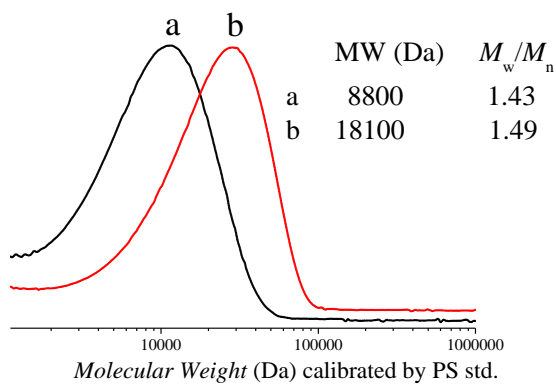


Figure S10: Plots showing the SEC outputs for the analysis of the PCL, synthesised as per the conditions above. Curve a is the first ϵ -CL polymerization (100 eq) and curve b shows the polymer after the second addition (100 eq) and polymerization of ϵ -CL.

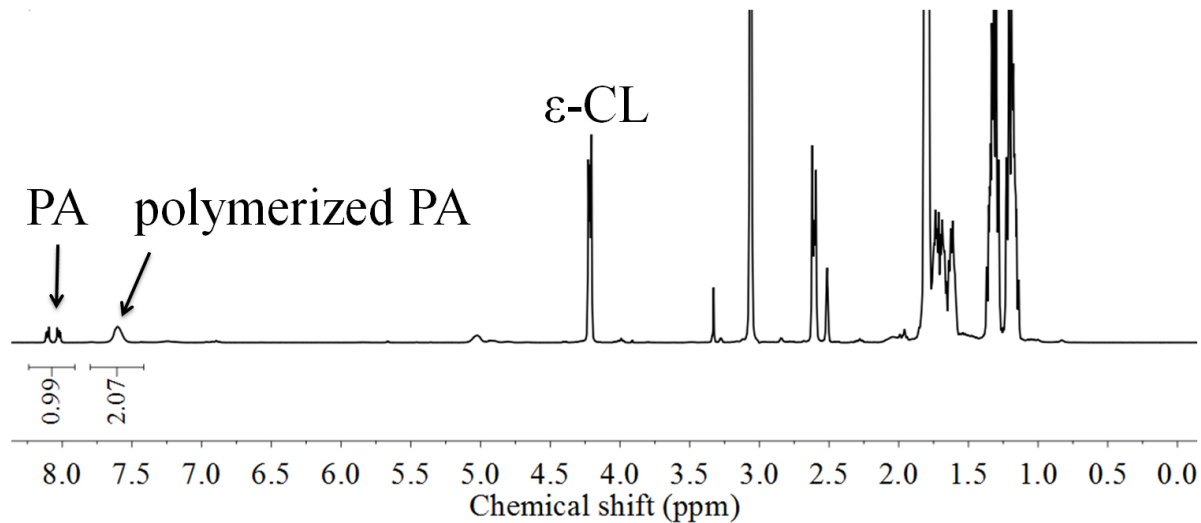


Figure S11: ^1H NMR spectrum showing selective formation of PCHPE with no polymerization of PCL. Reaction conditions from Table 2, entry 4.

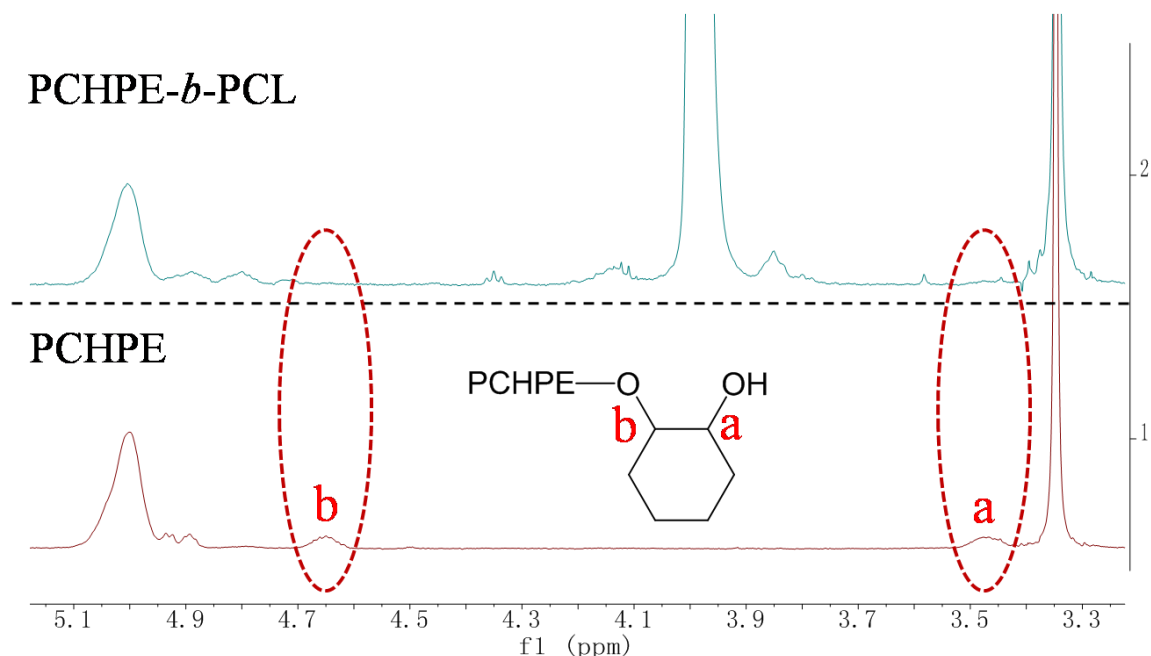


Figure S12: ^1H NMR spectra of the PCHPE block and, subsequently, the PCHPE-*b*-PCL block copolyester. Conditions as per Table 2, entry 2.

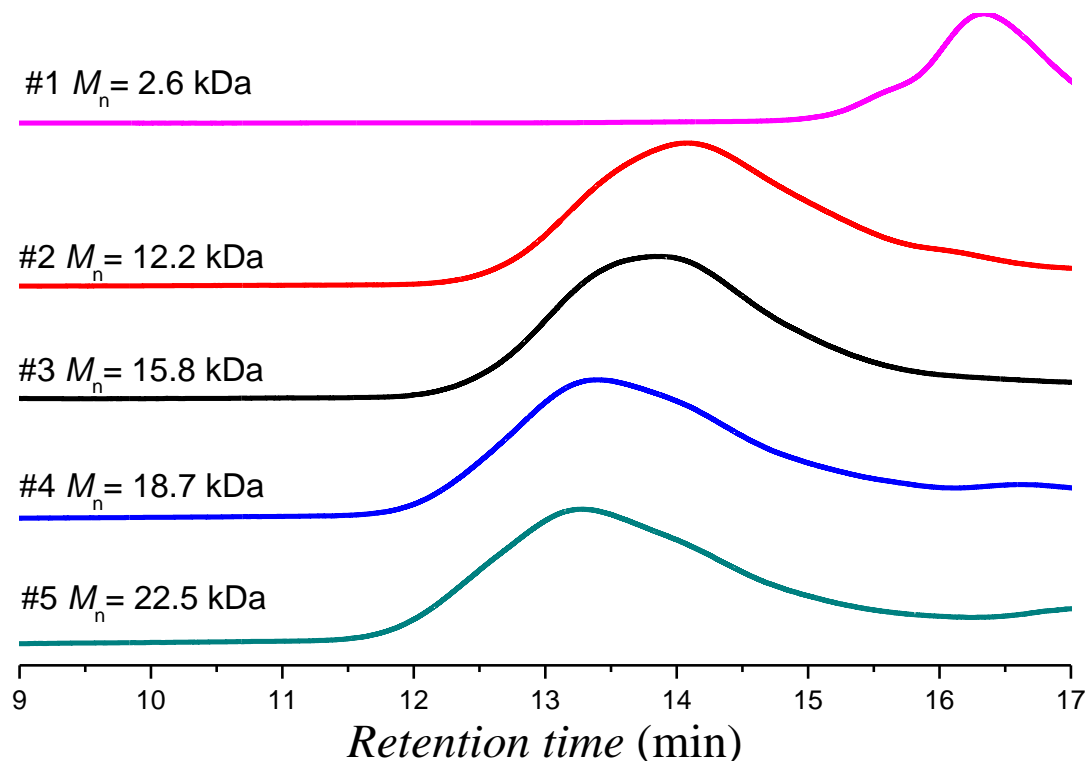


Figure S13: The SEC plots for polyesters (PCHPE-*b*-PCL and PCHPE). The chromatograms correspond to the relevant entries in Table 2.

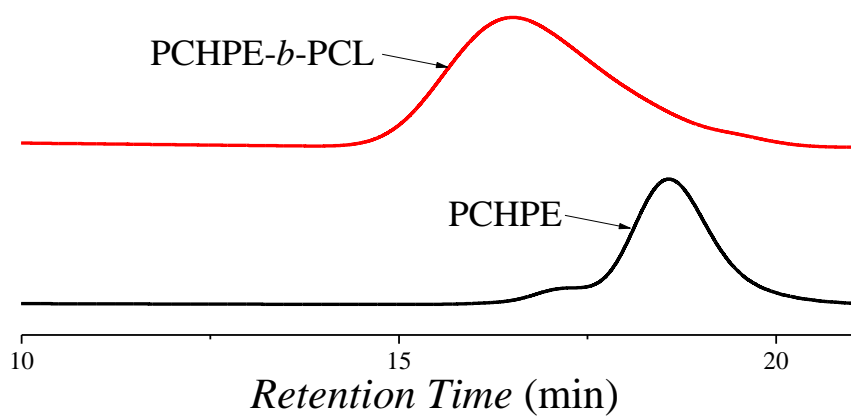


Figure S14. The SEC plots for polyesters, PCHPE (Table 2, entry 1) and PCHPE-*b*-PCL (Table 2, entry 3), recorded using a UV detector at 254 nm.

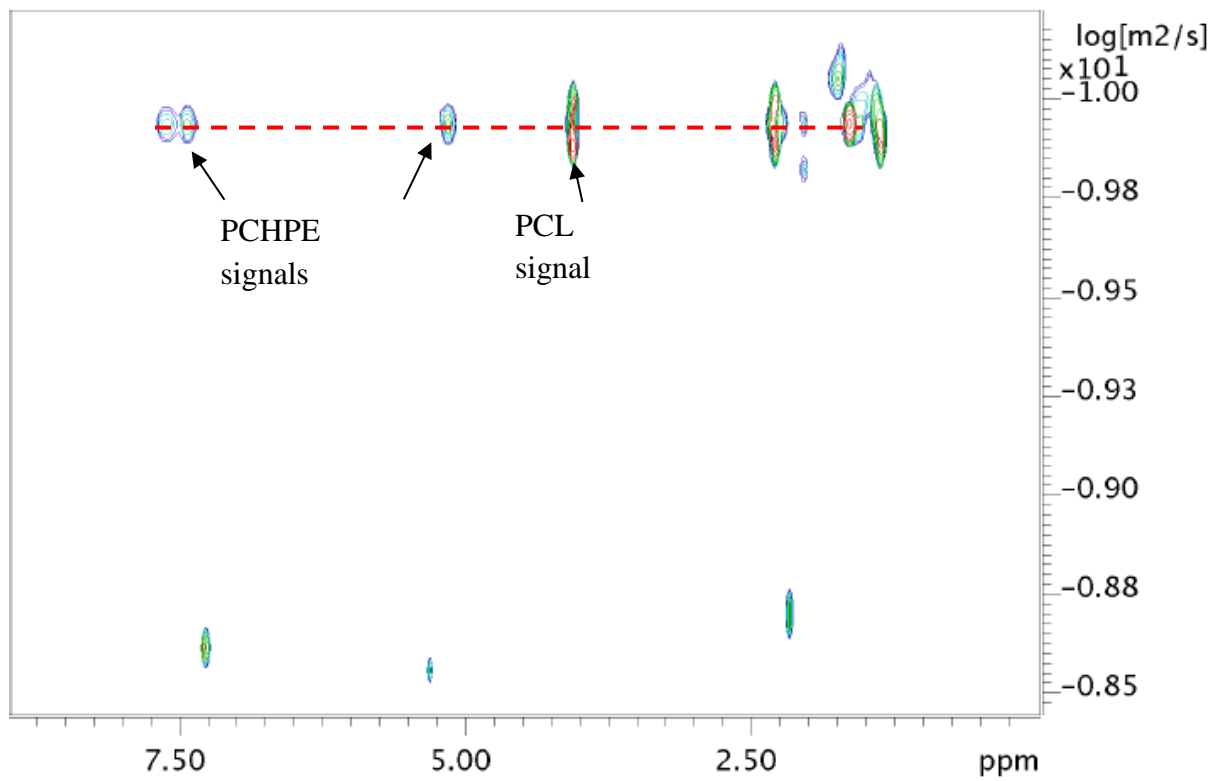


Figure S15: The DOSY spectrum of the block copolyester (PCHPE-*b*-PCL) prepared according to the conditions described in Table 2, entry 2.

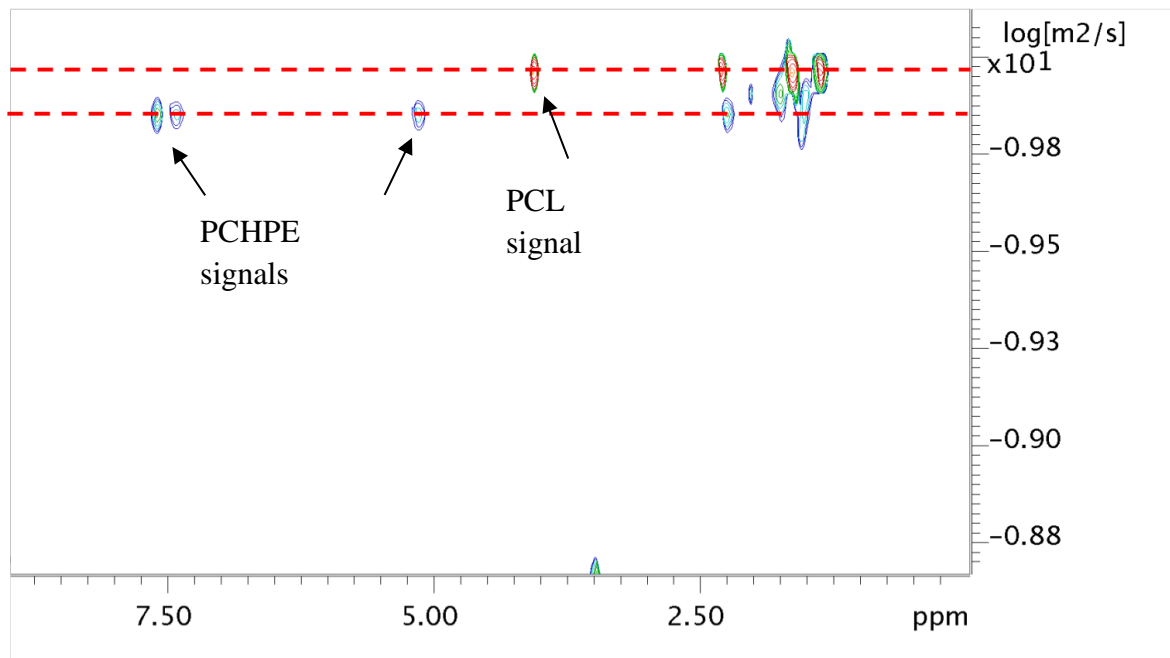


Figure S16: The DOSY spectrum of a mixture of PCHPE and PCL.

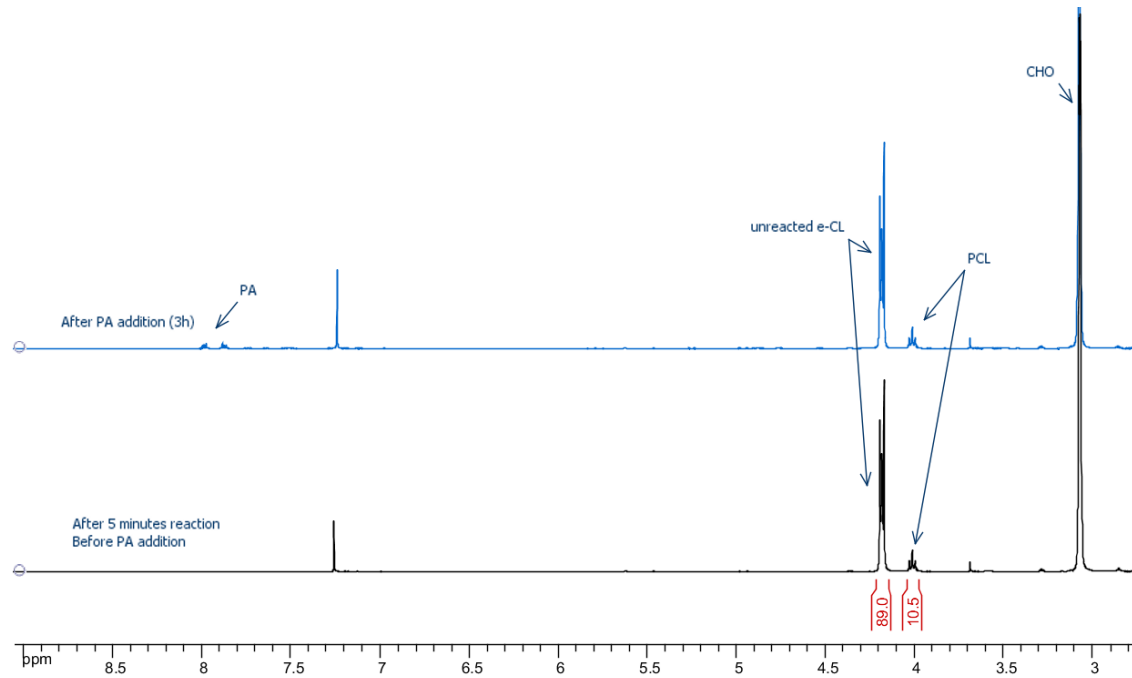


Figure S17: ^1H NMR spectra showing ϵ -CL ROP inhibition by the addition of PA. Reaction conditions: **1** $\text{CHO}/\epsilon\text{-CL} = 1/2000/600$, at 80°C , 5 min; then the addition of 20 eq. (vs. **1**) of PA.

Table S6: Data for the DFT calculations illustrated in Figures 10.

Structure	T (K)	ΔG	JobID	Link
6"	373.15		104128	http://dx.doi.org/10.6084/m9.figshare.1506861
eCL"	373.15		104285	http://dx.doi.org/10.6084/m9.figshare.1507558
6"+eCL"	373.15	0		
7"	373.15	3.3	104129	http://dx.doi.org/10.6084/m9.figshare.1507553
8CL"-TS	373.15	37	104264	http://dx.doi.org/10.6084/m9.figshare.1507559
9CL"	373.15	3.4	104131	http://dx.doi.org/10.6084/m9.figshare.1507557
10CL"-TS	373.15	19.4	104136	http://dx.doi.org/10.6084/m9.figshare.1507556
11CL"	373.15	15.2	104133	http://dx.doi.org/10.6084/m9.figshare.1507554
12CL"	373.15	10.7	104134	http://dx.doi.org/10.6084/m9.figshare.1507555
PA"	373.15		104337	http://dx.doi.org/10.6084/m9.figshare.1507562
6" + PA"	373.15	0		
7PA"	373.15	3.3	104293	http://dx.doi.org/10.6084/m9.figshare.1507563
8PA"-TS	373.15	18.8	104291	http://dx.doi.org/10.6084/m9.figshare.1507564
11PA"	373.15	-23.2	104292	http://dx.doi.org/10.6084/m9.figshare.1507565

DFT protocol: # rwb97xd/6-31g(d) scrf=(cpcm,solvent=dichloromethane) NoSymm temperature=373.15 K

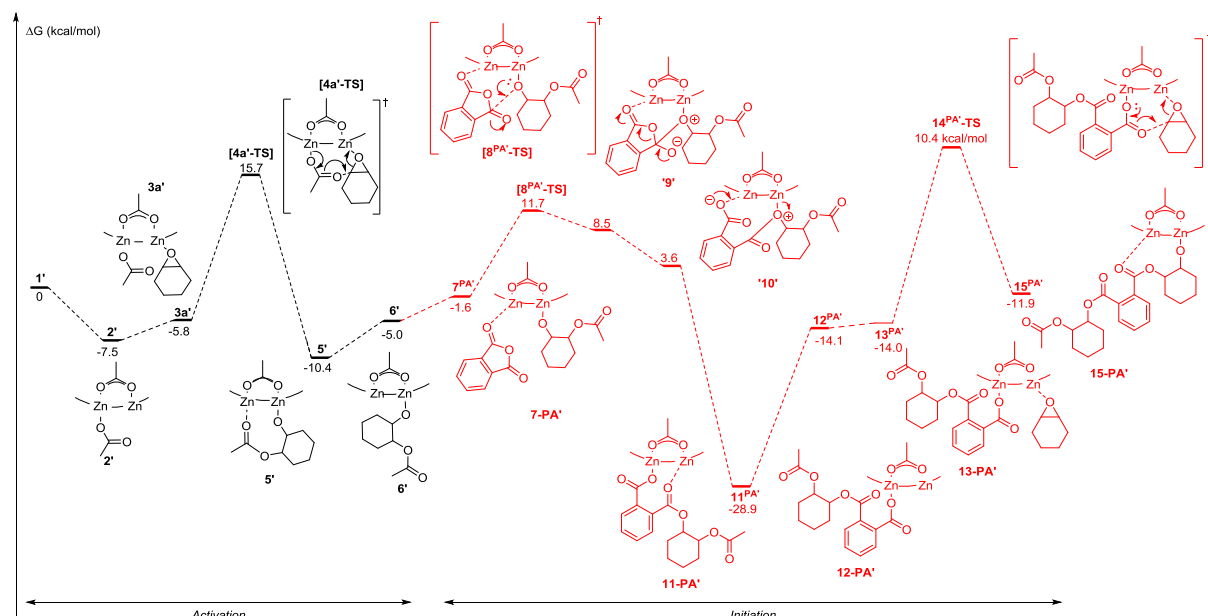


Figure S18: Illustrates the calculated potential energy surface for ROCOP of CHO/PA that includes two hidden intermediates between $8^{PA'-TS}$ and $11^{PA'}$. DFT protocol: # rwb97xd/6-31g(d) scrf=(cpcm,solvent=dichloromethane) NoSymm temperature=373.15K integral=grid=ultrafine. Data available at <http://doi.org/10.14469/hpc/281>.

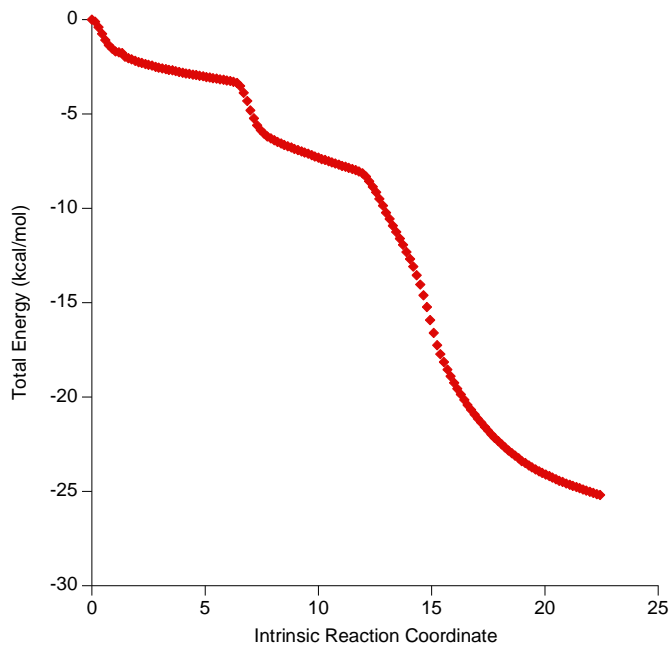


Figure S19: IRC calculations from 8PA'-TS. DFT protocol: # IRC = (reverse, maxpoints=150, recalc=10, calcfc, maxcycle=40, tight, cartesian, lqa, stepsize=15) wb97xd/6-31g(d); integral=grid=ultrafine; temperature = 373.15 K scrf=(cpcm,solvent=dichloromethane). Data available at <http://doi.org/10.14469/hpc/281>.

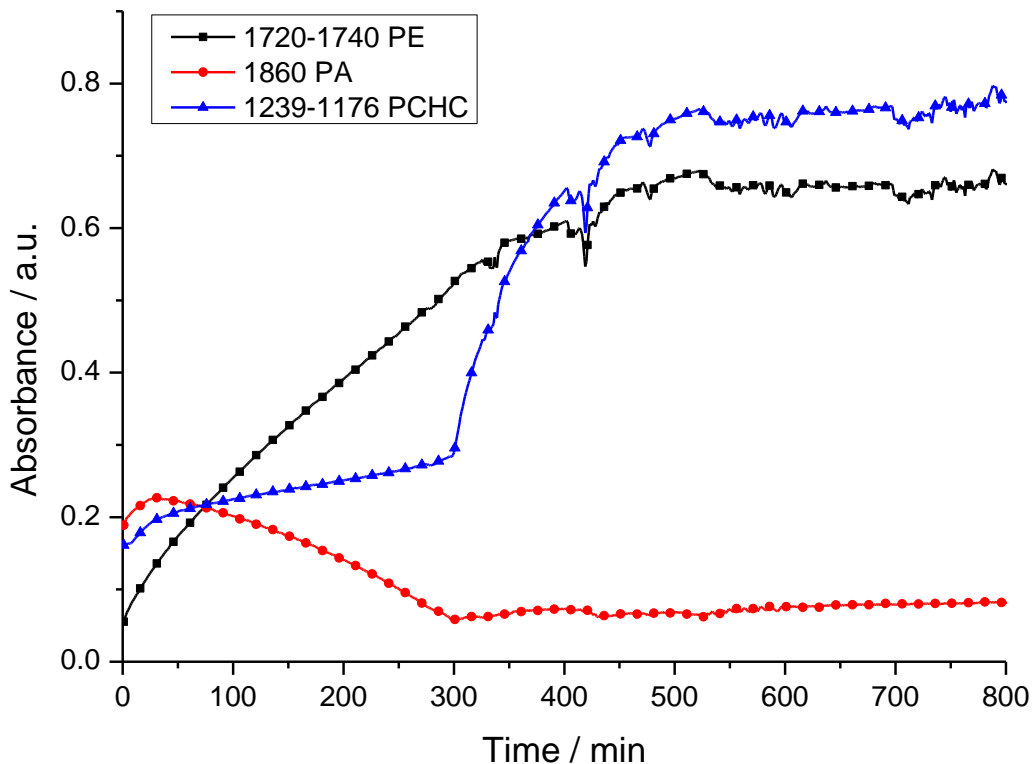


Figure S20: Shows the changes in the intensity of the ATR-FTIR resonances observed during ROCOP of PA, CHO and CO_2 using complex **1**. Polymerization conditions: **1**:PA:CHO = 1:10:800, under 1 bar CO_2 at 100 °C. The baseline ‘noise’ observed after 400 minutes results from an increase in sample viscosity due to polymerization reaching relatively higher conversions. The slight increase in PA concentration at very start is due to the time required for PA to fully dissolve in the CHO. Reproduced with permission from reference 6.

Table S7: Comparison of two different basis sets for selected intermediates for CHO/CO₂ ROCOP. An interactive version of this table can be found online at <http://doi.org/10.14469/hpc/331>.

Structure	ΔG^a [6-311G(d,p)] for C,H,O,N Zn: [6-311G(2df)]	Structure	ΔG^b [6-31G(d)] for all atoms
6' *	0	6'	0
7^{CO2''*}	+6.8	7^{CO2'}	+3.0
8^{TS-CO2''*}	+11.9	8^{TS-CO2'}	+12.8
10^{TS-CO2''*}	+12.81	10^{TS-CO2'}	+14.5

a) DFT protocol: # rwb97xd/ C,H,O,N:6-311G(d,p), Zn:6-311G(2df)
scrf=(cpcm,solvent=dichloromethane) NoSymm temperature=353.15 K; b) # rwb97xd/6-31g(d)
scrf=(cpcm,solvent=dichloromethane) NoSymm temperature=353.15 K

Table S8: Comparison of two different basis sets for selected intermediates for CHO/PA ROCOP. An interactive version of this table can be found online at <http://doi.org/10.14469/hpc/332>.

Structure	ΔG^a [[6-311G(d,p)] for C,H,O,N Zn: [6-311G(2df)]	Structure	ΔG^b [6-31G(d)] for all atoms
6' *	0	6' *	0
7^{PA''*}	+1.9	7^{PA''*}	+3.4
8^{TS-PA''*}	+16.5	8^{TS-PA''*}	+16.7
11^{TS-PA''*}	-25.5	11^{TS-PA''*}	-23.9

a) DFT protocol: # rwb97xd/ C,H,O,N:6-311G(d,p), Zn:6-311G(2df)
scrf=(cpcm,solvent=dichloromethane) NoSymm temperature=373.15 K; b) # rwb97xd/6-31g(d)
scrf=(cpcm,solvent=dichloromethane) NoSymm temperature=373.15 K

NMR data and SEC data for entries in Table 1

Table 1, Entry 1:

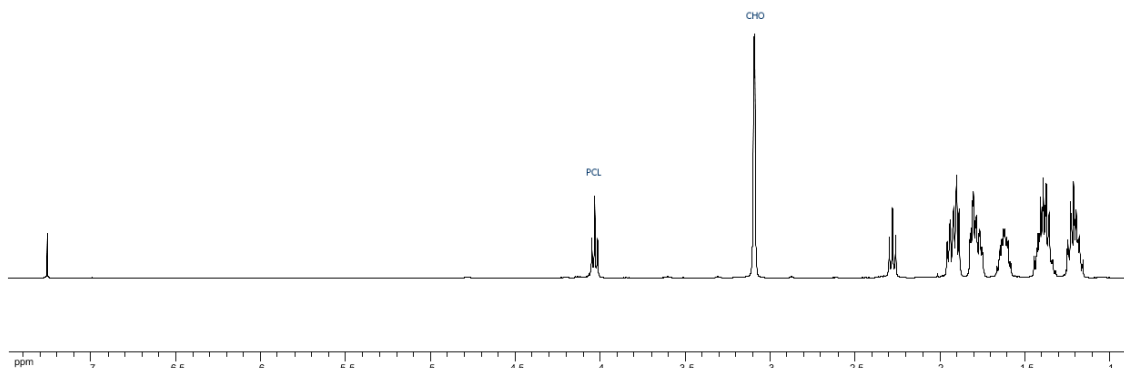
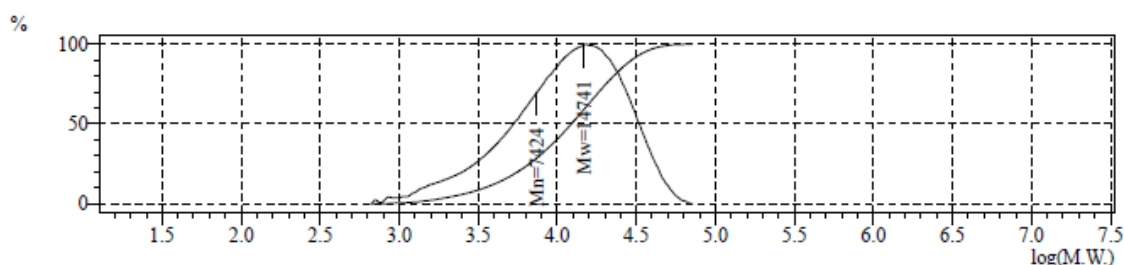


Figure S21: ^1H NMR spectrum showing full conversion of ε -CL to PCL in CHO, Table 1, entry 1



Detector A Channel 1

Peak#	Ret. Time	Area	Height	Conc.	Name
1	15.604	561023	2333	0.000	
Total		561023	2333		

Peak#:1 (Detector A Channel 1)
[Average Molecular Weight]

Mn 7424 Mw 14741 Mw/Mn 1.99 % 100.0

Figure S22: Plots showing the SEC outputs for the analysis of the PCL, Table 1, entry 1.

Table 1, Entry 2

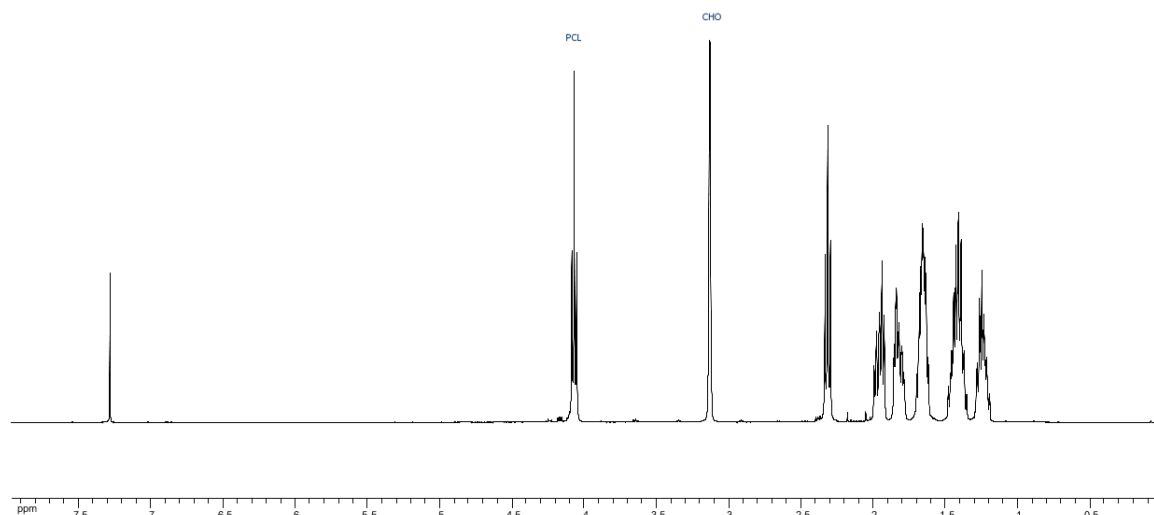


Figure S23: ^1H NMR spectrum showing full conversion of e-CL to PCL in CHO, Table 1, entry 2

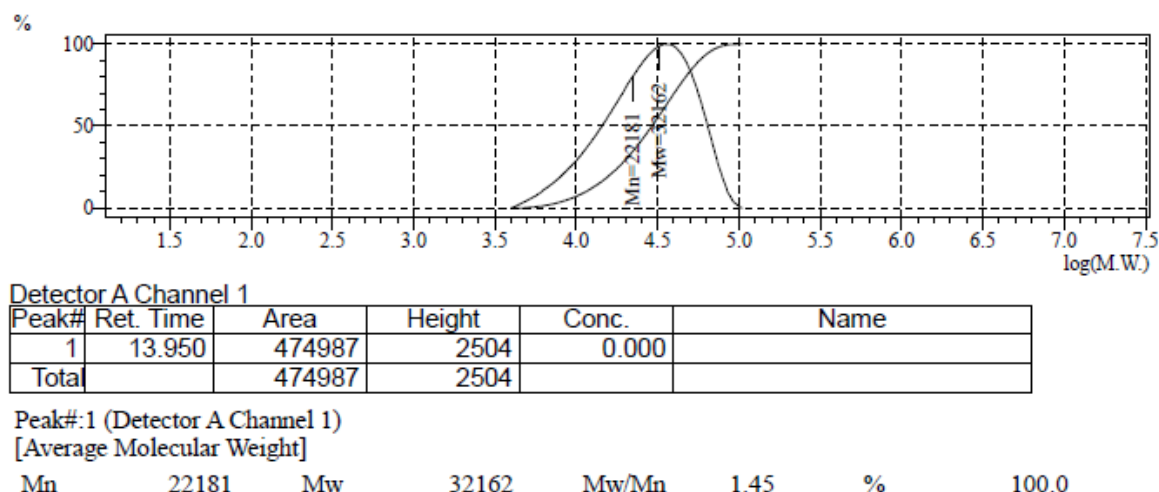


Figure S24: Plots showing the SEC outputs for the analysis of the PCL, Table 1, entry 2.

Table 1, Entry 3

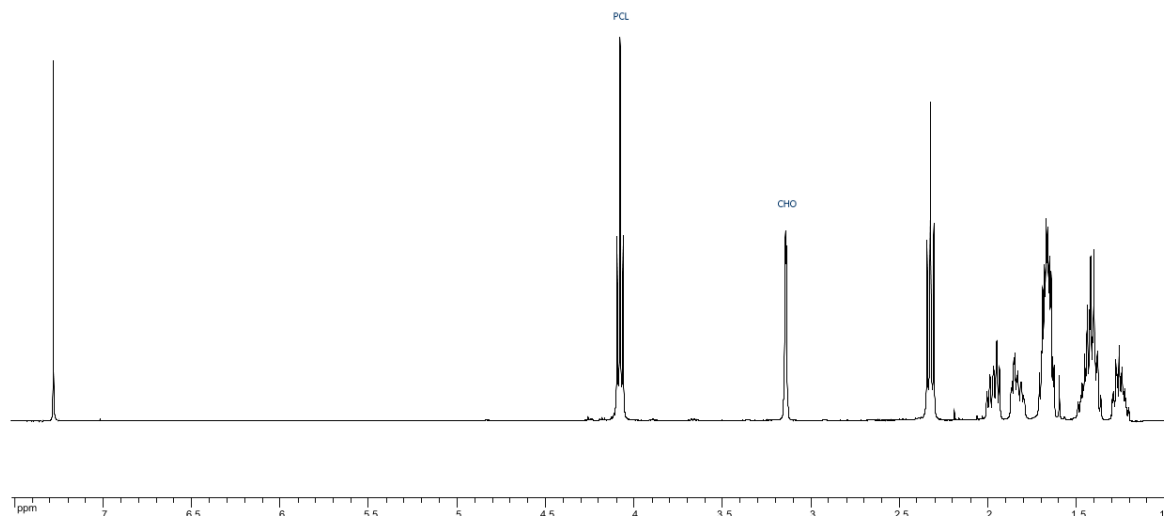
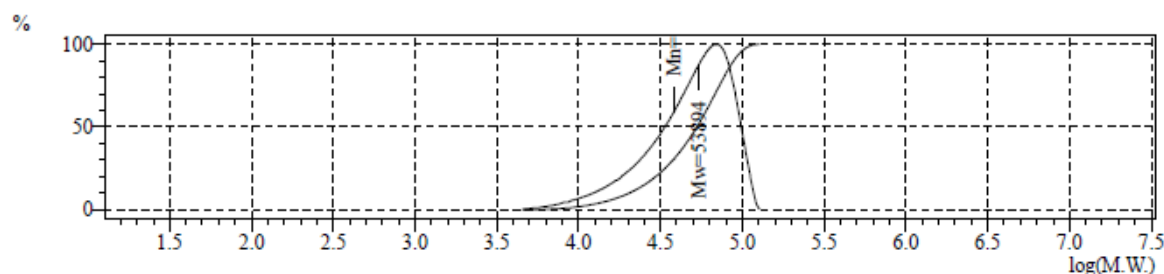


Figure S25 ¹H NMR spectrum showing full conversion of ε -CL to PCL in CHO, Table 1, entry 3



Detector A Channel 1

Peak#	Ret. Time	Area	Height	Conc.	Name
1	12.487	574089	3896	0.000	
Total		574089	3896		

Peak#:1 (Detector A Channel 1)
[Average Molecular Weight]

Mn 38072 Mw 53894 Mw/Mn 1.42 % 100.0

Figure S26: Plots showing the SEC outputs for the analysis of the PCL, Table 1, entry 3.

Table 1, Entry 4

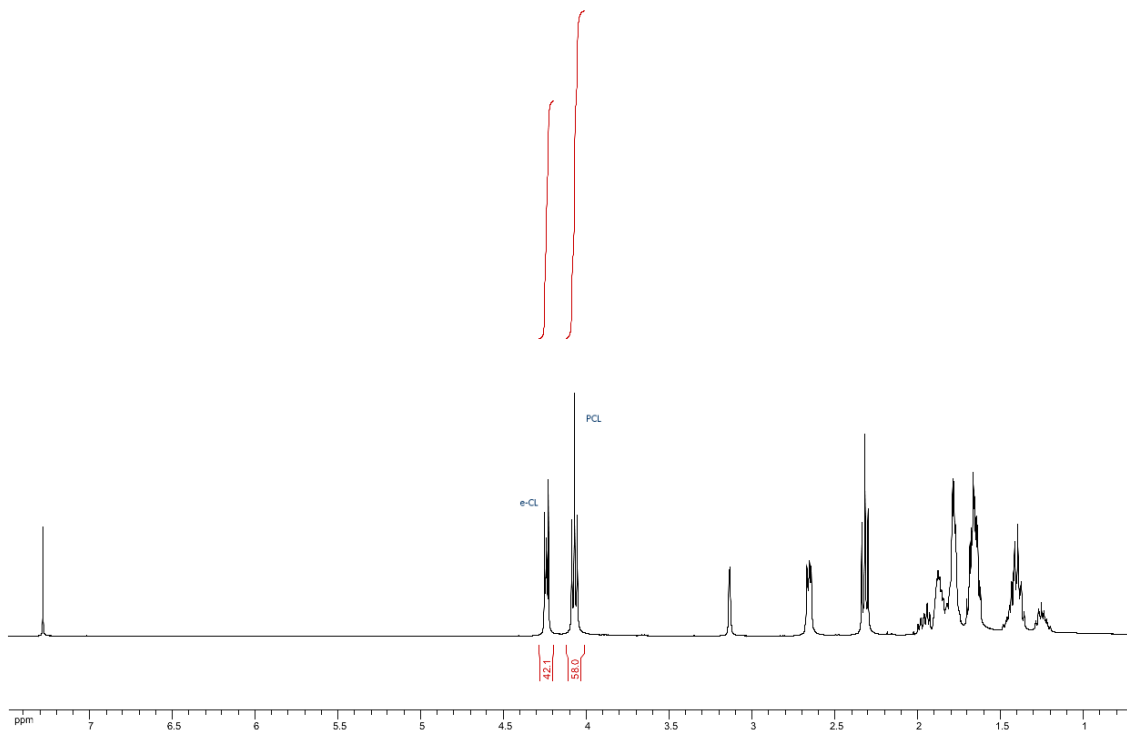


Figure S27: ¹H NMR spectrum showing 58% conversion of ε -CL to PCL in CHO, Table 1, entry 4

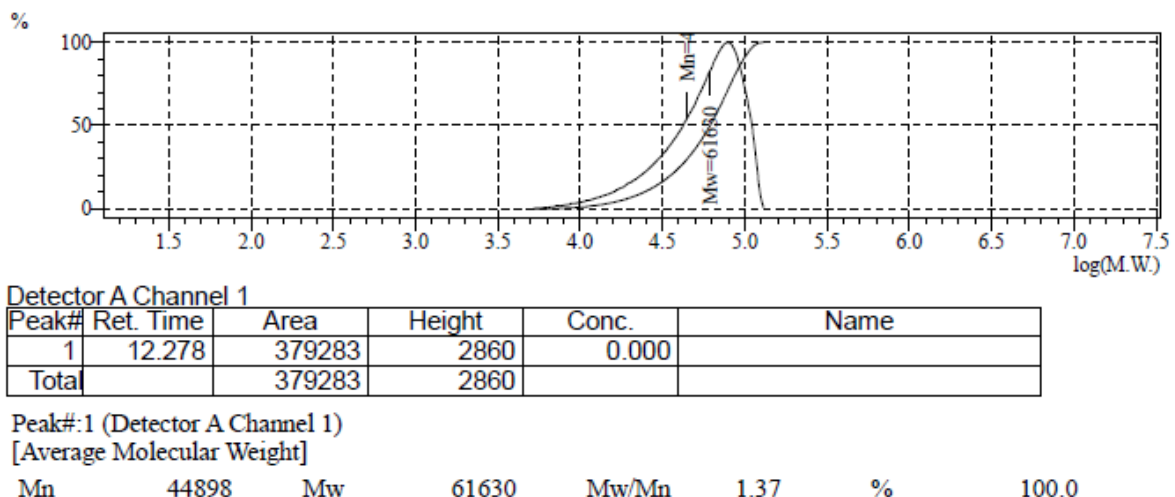


Figure S28: Plots showing the SEC outputs for the analysis of the PCL, Table 1, entry 4.

NMR data for Table 2

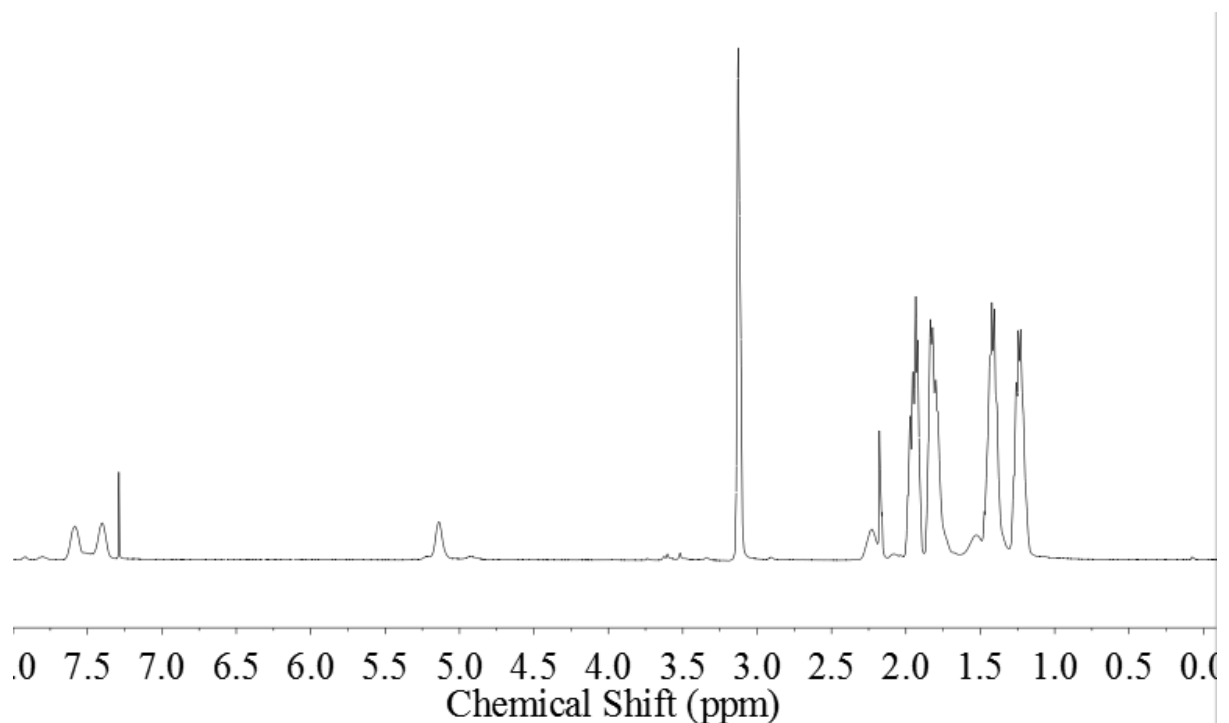


Figure S29: ^1H NMR spectrum of Table 2, entry 1 in CDCl_3

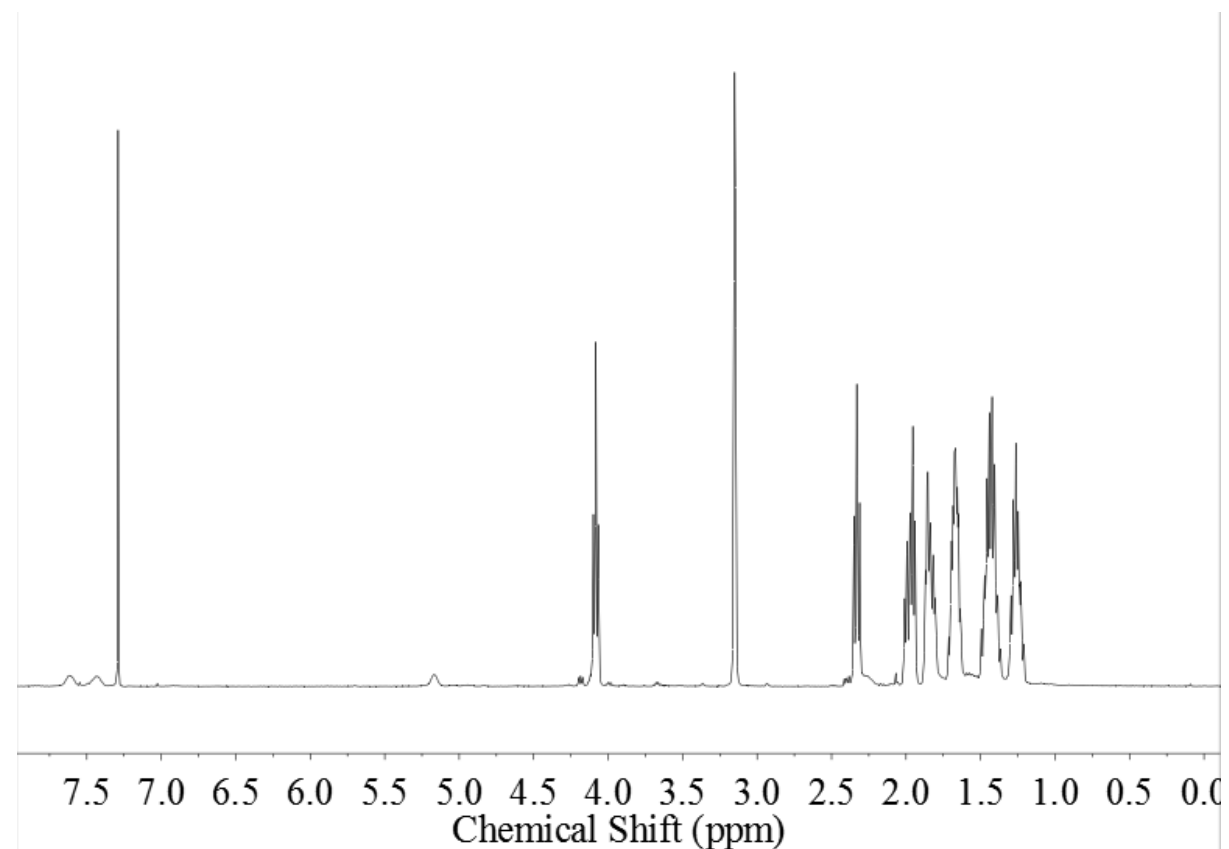


Figure S30: ^1H NMR spectrum of Table 2, entry 2 in CDCl_3

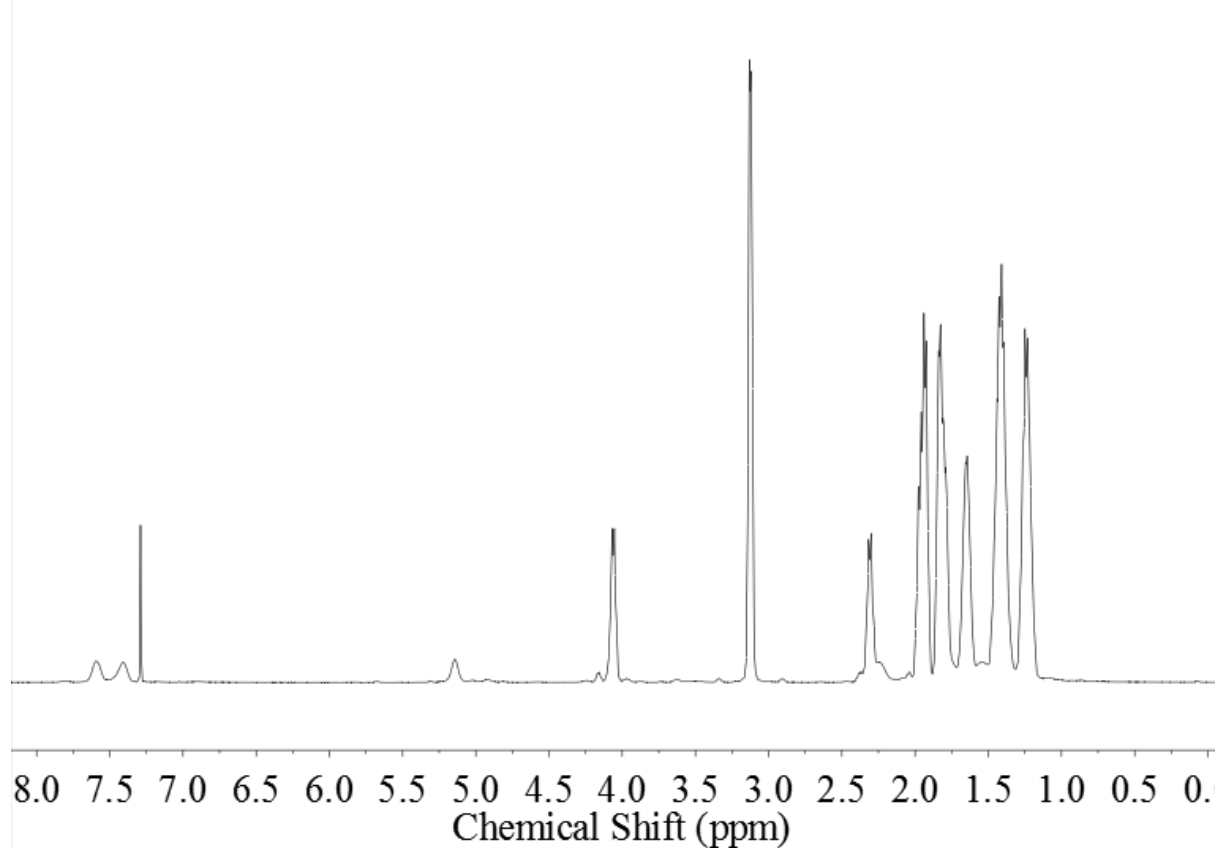


Figure S31: ^1H NMR spectrum of Table 2, entry 3 in CDCl_3

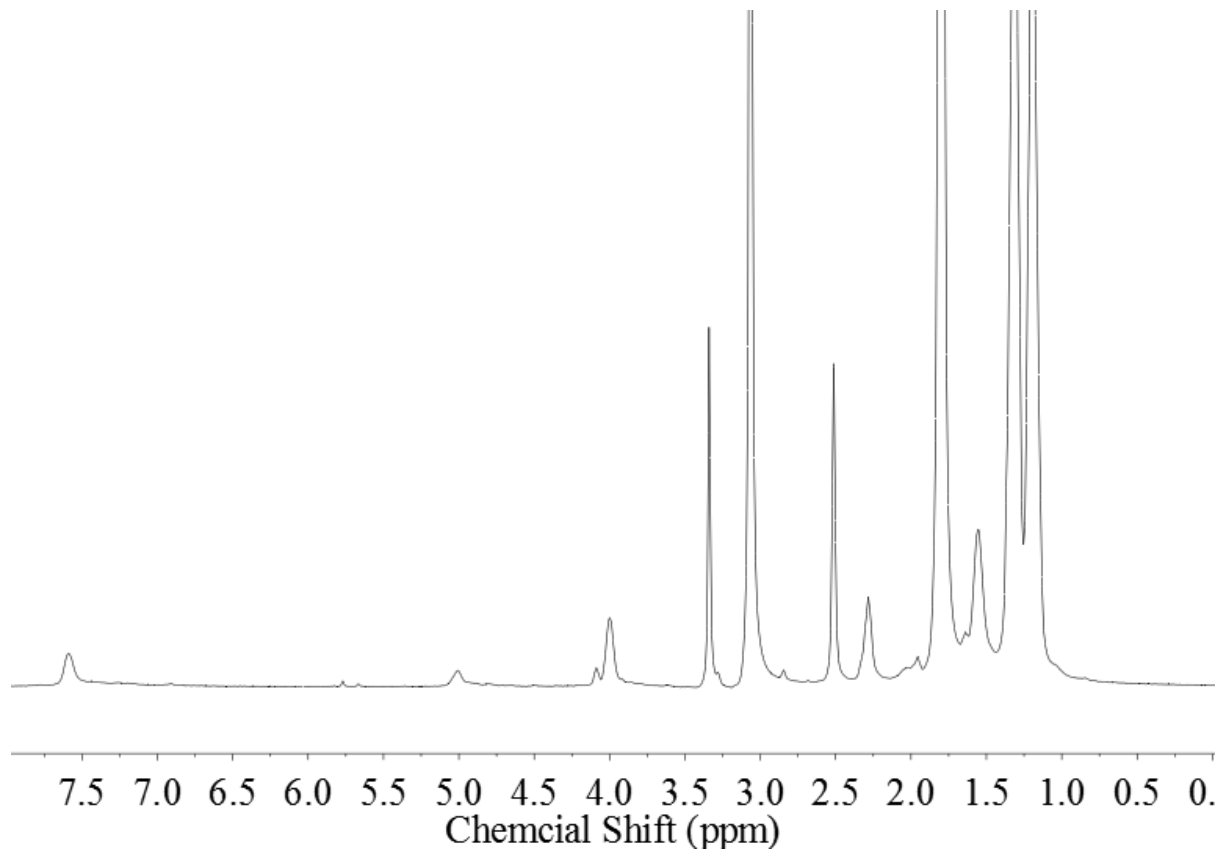


Figure S32: ^1H NMR spectrum of Table 2, entry 4 in DMSO-d_6

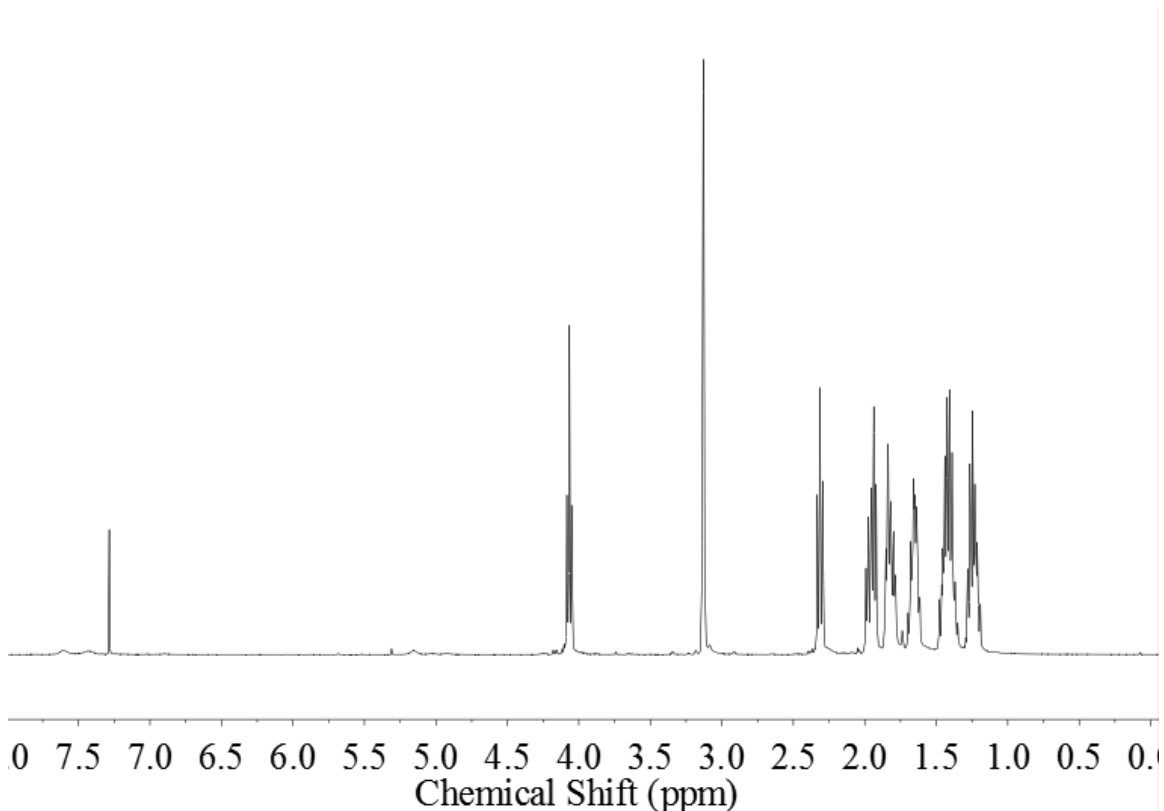


Figure S33: ^1H NMR spectrum of Table 2, entry 5 in CDCl_3

REFERENCES

1. Romain, C.; Williams, C. K. *Angew. Chem. Int. Ed.* **2014**, *53*, 1607-1610.
2. Jutz, F.; Buchard, A.; Kember, M. R.; Fredrickson, S. B.; Williams, C. K. *J. Am. Chem. Soc.* **2011**, *133*, 17395–17405.
3. Gaussian 09, Revision A.1, Frisch, M. J.; Trucks, G. W.; Schlegel, H. B.; Scuseria, G. E.; Robb, M. A.; Cheeseman, J. R.; Scalmani, G.; Barone, V.; Mennucci, B.; Petersson, G. A.; Nakatsuji, H.; Caricato, M.; Li, X.; Hratchian, H. P.; Izmaylov, A. F.; Bloino, J.; Zheng, G.; Sonnenberg, J. L.; Hada, M.; Ehara, M.; Toyota, K.; Fukuda, R.; Hasegawa, J.; Ishida, M.; Nakajima, T.; Honda, Y.; Kitao, O.; Nakai, H.; Vreven, T.; Montgomery, Jr., J. A.; Peralta, J. E.; Ogliaro, F.; Bearpark, M.; Heyd, J. J.; Brothers, E.; Kudin, K. N.; Staroverov, V. N.; Kobayashi, R.; Normand, J.; Raghavachari, K.; Rendell, A.; Burant, J. C.; Iyengar, S. S.; Tomasi, J.; Cossi, M.; Rega, N.; Millam, N. J.; Klene, M.; Knox, J. E.; Cross, J. B.; Bakken, V.; Adamo, C.; Jaramillo, J.; Gomperts, R.; Stratmann, R. E.; Yazyev, O.; Austin, A. J.; Cammi, R.; Pomelli, C.; Ochterski, J. W.; Martin, R. L.; Morokuma, K.; Zakrzewski, V. G.; Voth, G. A.; Salvador, P.; Dannenberg, J. J.; Dapprich, S.; Daniels, A. D.; Farkas, Ö.; Foresman, J. B.; Ortiz, J. V.; Cioslowski, J.; Fox, D. J. Gaussian, Inc., Wallingford CT, 2009.
4. Buchard, A.; Jutz, F.; Kember, M. R.; White, A. J. P.; Rzepa, H. S.; Williams, C. K. *Macromolecules* **2012**, *45*, 6781-6795.
5. Kowalski, A.; Duda, A.; Penczek, S. *Macromolecules* **1998**, *31*, 2114-2122.
6. Saini, P. K.; Romain, C.; Zhu, Y.; Williams, C. K. *Polym. Chem.* **2014**, *5*, 6068-6075.